Ultra Wideband In Vivo Channel Modelling with Respect to Ex Vivo Antenna Location

Muhammad Ilyas[1], Oguz Bayat[1], Muhammad Ali Imran[2], Qammer H. Abbasi[2]
[1]School of Engineering and Natural Sciences, Altinbas University, Istanbul, Turkey, ilyas8787@gmail.com
[2]School of Engineering, University of Glasgow, Glasgow, UK, qammer.abbasi@glasgow.ac.uk

***Abstract*—This article presents mathematical channel modeling for *in-vivo* communication in terms of the change in the position of the *ex-vivo* antenna at ultra wideband frequencies. It is shown that the location dependent characteristics are not only dependent on the *in-vivo* devices placed inside the human body but also the position of *ex-vivo* devices can impact the channel. Results are calculated using the mathematical model and curve fitting technique by calculation of the Root Mean Square Error (RMSE). The statistics of error prediction among the measured data and the proposed model is RMSE = 14.46 for the right lateral and RMSE = 11.63 for the left lateral respectively. These results will help system designer in accurate link budget calculation for designing enhance implantable devices.**

***Index Terms*—antenna propagation, ex-vivo, implantable devices, in-vivo channel, measurement data.**

I. INTRODUCTION

Channel characteristics, utilization, estimation and modeling are under research for *in*-vivo communication from few years [1]. Those analyses will help us re design the future of medical world and the communication between the doctors and patients are expected to be more reliable than ever before. It will also help us in chronic diseases which need to be identified before or on time to respond it quickly. Most of the patient's loss their lives because of the delayed response from the medical team, especially if someone is having heart attack while sleeping. In order to overcome those types of serious diseases and respond it on time, we need to advance our research for implantable devices and study the *in-vivo* communication and its channel to make it possible to communicate with conventional devices using Wi-Fi, 3G, 4G and now 5G spectrum which can be used to inform the medical team automatically in case of an emergency.

An overview of the future of medical devices is presented in [2], where the authors also presented an overview of the current *in-vivo* antennas their shapes, size and functions. Experimental analysis is also performed using a human cadaver torso by placing fresh organs of sheep at 915 MHz [3], those analyses are believed to be the first of its kind by the authors and have the most efficient results so far. As performing tests using a living human body is hard and not ethical the best and closest tests to resemble the real scenario as much as possible is to use a human cadaver. The *in-vivo* channel response for heart, stomach and intestine is also presented in [4] at Ultra-Wideband (UWB). The authors showed the location dependent characteristics of the channel along with how the channel is getting impacted while changing the position of the *in*-vivo antennas while the position of the *ex*-vivo antennas was fixed.

The *in-vivo* channel was studied multiple times using different simulations and experiments and number of different model using different techniques can be found in the literature. This includes an on body radio channel characteristics and modeling for Orthogonal Frequency Division Multiplexing (OFDM) at UWB [5] for the body centric wireless networks. Numerical characteristics and modeling is presented in [6], Followed by UWB channel model in [7] and system level modeling of optimal UWB body centric networks [8]. All the model has their own way of presentation and modeling the channel. The common thing in the presentation of those models are that for each of those studies UWB is considered and the reason is to achieve high data rates by exploiting the wide band characteristics of the channel with minimum or no delay.

In [9] the authors present a mathematical model using the measurement data collected from the experiments at UWB along with the derivation of the model. The model presented is only efficient if the position of the *ex-vivo* antenna is fixed, i.e. no movement or position change for the external device/antenna. The performance evaluation of the channel is presented in [10].

In this paper, we show the channels using the measurement data by moving the *ex-vivo* antenna from the right lateral to the left lateral. The models for both the measurements are presented along with the RMSE for right and left lateral.

II. ANTENNA PLACEMENT BESIDES RIGHT AND LEFT LATERAL

The measurement setup and placement of the *ex-vivo* antenna can be seen in Fig. 1. Torso part of the human cadaver is used for all the experiments. The detailed information regarding the experiments and devices used in the experiments can be found in [4] along with the placement of the *in-vivo* antenna. The *ex-vivo* antenna is connected with the Vector Network Analyzer (VNA) through a 2 meters long coaxial cable is initially placed besides the right lateral and the readings were taken. The same antenna with the same setup is than moved towards the left lateral and all the readings were taken, while the *in-vivo* antenna was placed inside the torso and the position of the antenna was fixed. All the readings are further processed in MATLAB©.

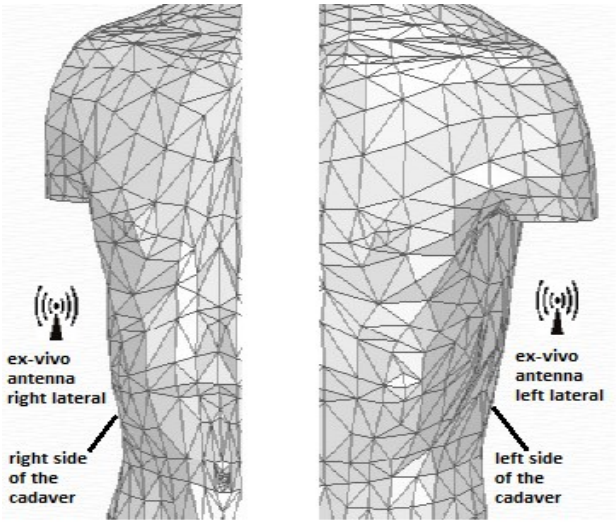

Fig. 1. Placement of the ex vivo antenna at right and left lateral

The channel response for the measurement data by placing the *ex*-vivo antenna near right lateral is shown in Fig. 2. The mathematical model is extracted using the 8 terms Fourier series representation having sines and cosines in the general form of the equation as (1). The derivation used for the extraction of the general form is presented in [9]. The general form is used to derive the new channel model by placing the *ex-vivo* antenna near the right and left lateral of the human torso.

$$f_x = a_o + \sum_{n=1}^{8} a_n \cos(n * x * w) + \sum_{n=1}^{8} b_n \sin(n * x * w) \quad (1)$$

Where, a_o, a_n and b_n represents the coefficients and w represents the weight in the equation.

The values of the coefficients for the 8 terms equation is presented in Table I along with the 95% confidence bounds for each coefficient in the equation calculated using MATLAB©.

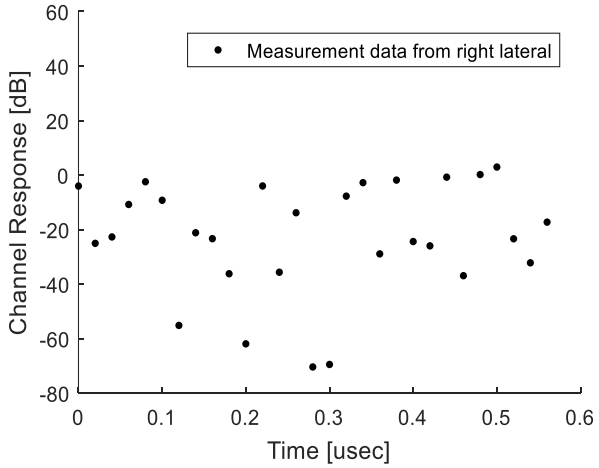

Fig. 2. Channel response for right lateral.

TABLE I. COEFFICIENT VALUES AND 95% CONFIDENCE LIMITS (RIGHT LATERAL)

Coefficient		**95% Confidence Limits**	
a_o		-24.71 (-30.96, -18.47)	
a_n	***Value (Limits)***	b_n	***Value (Limits)***
a_1	11.87 (2.899, 20.85)	b_1	5.339 (-3.457, 14.13)
a_2	1.008 (-7.832, 9.848)	b_2	-2.669 (-11.67, 6.33)
a_3	-9.32 (-18.09, -0.5503)	b_3	-4.71 (-15.2, 5.78)
a_4	7.908 (-1.063, 16.88)	b_4	7.908 (-1.063, 16.88)
a_5	12.01 (0.779, 23.25)	b_5	-9.744 (-22.43, 2.942)
a_6	-0.709 (-9.392, 7.974)	b_6	1.817 (-7.381, 11.02)
a_7	-8.641 (-19.26, 1.976)	b_7	5.084 (-8.14, 18.31)
a_8	5.686 (-6.513, 17.88)	b_8	7.353 (-3.246, 17.95)

All the values presented in Table I are used in (1) to come up with the final proposed fitted mode for the experimental channel as shown in Fig. 3. While the residual plot is presented in Fig. 4.

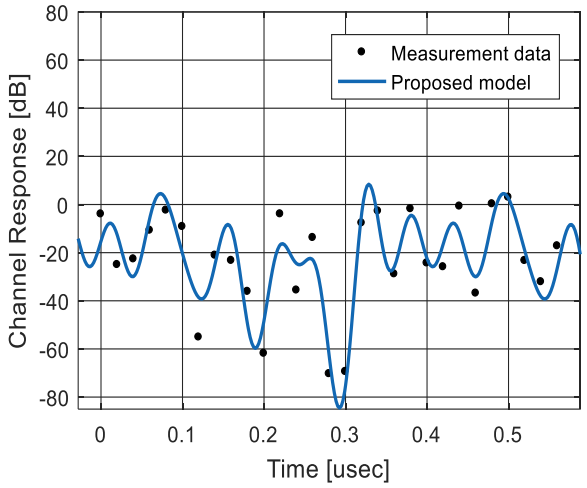

Fig. 3. Porposed model for experimental channel (right lateral)

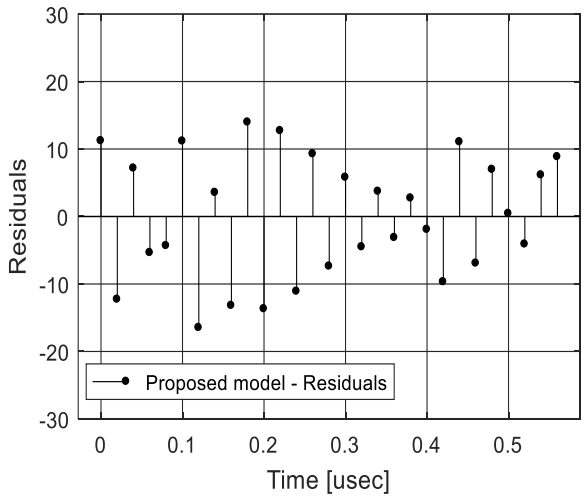

Fig. 4. Residual plot (right lateral)

The channel response for the experimental data by placing the *ex-vivo* antenna near the left lateral is presented in Fig. 5. The values for the coefficinets of equation (1) is presented in Table II along with 95% confidence limits for each coefficient.

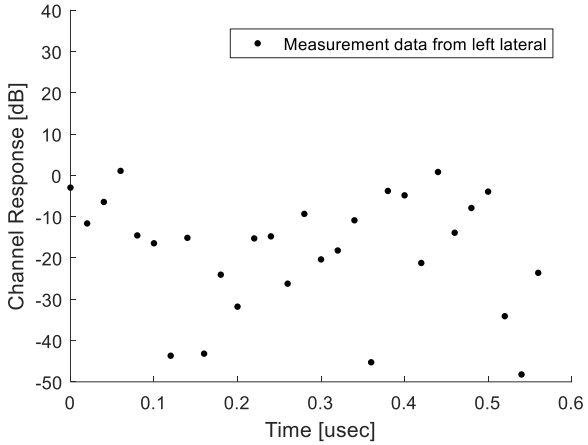

Fig. 5. Channel response for left lateral.

TABLE II. COEFFICIENT VALUES AND 95% CONFIDENCE LIMITS (LEFT LATERAL)

Coefficient		**95% Confidence Limits**	
a_o		-18.58 (-23.45, -13.71)	
a_n	***Value (Limits)***	b_n	***Value (Limits)***
a_1	-15.12 (-78.82, 48.57)	b_1	14.13 (-31.06, 59.32)
a_2	2.827 (-30.81, 36.46)	b_2	6.219 (-24.13, 36.57)
a_3	1.661 (-14.61, 17.93)	b_3	8.494 (-27.75, 44.74)
a_4	-5.229 (-70.53, 60.08)	b_4	10.71 (-29.5, 50.93)
a_5	13.22 (-53.69, 80.12)	b_5	-1.433 (-37.32, 34.45)
a_6	0.8734 (-20.37, 22.12)	b_6	8.343 (-31.54, 48.23)
a_7	-0.1388 (-38.08, 37.8)	b_7	8.585 (-34.36, 51.53)
a_8	13.89 (-66.73, 94.51)	b_8	-2.882 (-52.82, 47.06)

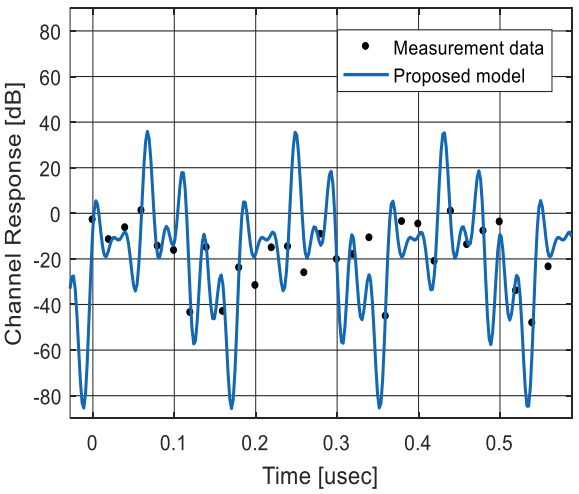

Fig. 6. Proposed model for experimental channel (left lateral)

The porposed fitted model can be seen in Fig. 6 while the *ex-vivo* antenna was placed near the left lateral. The residual plot for the fitted model is presented in Fig. 7.

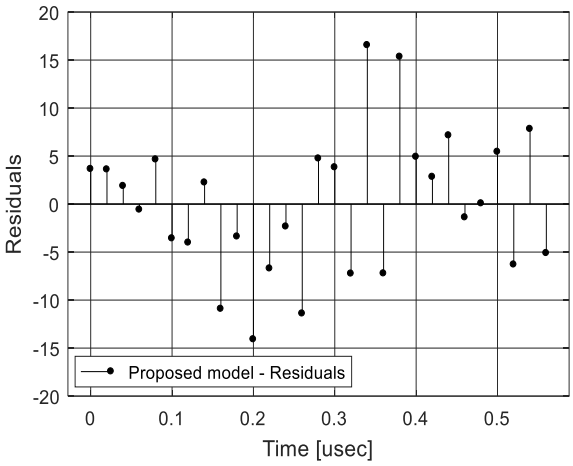

Fig. 7. Residual plot (left lateral)

III. COMPARISON OF THE MODELS AND RESULTS

Two different models are presented in this paper in terms of placing the antennas near right lateral and placing the antenna near left lateral. The statistical comparison for both the models are presented in Table III. It can be clearly seen from the figures and data presented in tables that the channel response while the antenna is placed near the right lateral is comparatively worst as compare to the left lateral. It can be because of the structure of the room. As in indoor structures the placement of equipment's along with the general stuff present in the room i.e. table, chair, desk, can also impact the channel. Those channels can also get an impact by the number of people present in the room at the time of measurement and their location. For these kind of readings one need to be careful enough by considering all the possible hurdles which can result in reflecting the signal and producing the multipath effect.

TABLE III. GOODNESS OF FIT

Right lateral		**Left lateral**	
SSE	2300	SSE	1488
R-squared	0.8086	R-squared	0.7307
Adjusted R-sqaured	0.5127	Adjusted R-sqaured	0.3145
RMSE	14.46	RMSE	11.63
Weights	14.93	Weights	34.54

IV. CONLUSION

This paper presented the possible mathematical model for the *in-vivo* communication with respect to changing the position of the antenna which was initially placed near the right lateral of the human torso and was shifted to the position near the left lateral of the human torso while the *in-vivo* antenna was placed inside the torso and the position was fixed.

The results proof the location dependent characteristics of the channel for the body centric devices and implants. Those results can help designers while designing the implantable devices for human body to consider not only the position and placement of the implantable device but also the environment where the device will be communicating with the outside world through any type of conventional communication device. The RMSE is also presented for both the models which can help the researcher to avoid extensive and time consuming experiments using human cadaver. They can directly use our model for their analysis by considering the RMSE for each model.

REFERENCES

[1] Qammer H. Abbasi, Masood Ur Rehman, Khalid Qaraqe and Akram Alomainy,"Advances in Body-Centric Wireless Communications: Applications and State-of-the-art", The Institution of Engineering and Technology (IET) Publication, July, 2016, ISBN: 978-1-84919-989-6 (print), ISBN 978-1-84919-990-2.

[2] A. F. Demir *et al*., "In Vivo Communications: Steps Toward the Next Generation of Implantable Devices," in *IEEE Vehicular Technology Magazine*, vol. 11, no. 2, pp. 32-42, June 2016.

[3] A. F. Demir, Q. H. Abbasi, Z. E. Ankarali, M. Qaraqe, E. Serpedin and H. Arslan, "Experimental Characterization of In Vivo Wireless Communication Channels," *2015 IEEE 82nd Vehicular Technology Conference (VTC2015-Fall)*, Boston, MA, 2015, pp. 1-2.

[4] M. Ilyas, O. Bayat and Q. H. Abbasi, "Experimental analysis of ultra wideband in vivo radio channel," *2018 26th Signal Processing and Communications Applications Conference (SIU)*, Izmir, 2018, pp. 1-4.

[5] Q. H. Abbasi, A. Sani, A. Alomainy and Y. Hao, "On-Body Radio Channel Characterization and System-Level Modeling for Multiband OFDM Ultra-Wideband Body-Centric Wireless Network," in *IEEE Transactions on Microwave Theory and Techniques*, vol. 58, no. 12, pp. 3485-3492, Dec. 2010.

[6] Q. H. Abbasi, A. Sani, A. Alomainy and Y. Hao, "Numerical Characterization and Modeling of Subject-Specific Ultrawideband Body-Centric Radio Channels and Systems for Healthcare Applications," in *IEEE Transactions on Information Technology in Biomedicine*, vol. 16, no. 2, pp. 221-227, March 2012.

[7] R. Di Bari, Q. H. Abbasi, A. Alomainy, and Y. Hao, "An Advanced UWB Channel Model for Body-Centric Wireless Networks, " *Progress In Electromagnetics Research*, Vol. 136, 79-99, 2013.

[8] A. Alomainy, Q. H. Abbasi, A. Sani and Y. Hao, "System-level modelling of optimal ultra wideband body-centric wireless network," *2009 Asia Pacific Microwave Conference*, Singapore, 2009, pp. 2188-2191.

[9] M. Ilyas, O. N. Ucan, O. Bayat, X. Yang and Q. H. Abbasi, "Mathematical Modeling of Ultra Wideband in Vivo Radio Channel," in *IEEE Access*, vol. 6, pp. 20848-20854, 2018.

[10] M. Ilyas, O. N. Ucan, O. Bayat, A. A. Nasir, M. A. Imran, A. Alomainy and Q. H. Abbasi, "Evaluation of Ultra-Wideband In-vivo Radio Channel and its Effects on System Performance," in *Transactions on Emerging Telecommunications Technologies*, Aug, 2018. (in press)